Redox Biology 66 (2023) 102860

Contents lists available at ScienceDirect

Redox Biology

journal homepage: www.elsevier.com/locate/redox

LRRK2 aggravates kidney injury through promoting MFN2 degradation and abnormal mitochondrial integrity

Shun Zhang [a,1], Subo Qian [a,**,1], Hailong Liu [a], Ding Xu [a], Weimin Xia [a], Huangqi Duan [a], Chen Wang [a], Shenggen Yu [a], Yingying Chen [b], Ping Ji [b], Shujun Wang [b], Xingang Cui [a,***], Ying Wang [b,****], Haibo Shen [a,*]

[a] Department of Urology, Xinhua Hospital, School of Medicine, Shanghai Jiao Tong University, Shanghai 200092, China
[b] Shanghai Institute of Immunology, Department of Immunology and Microbiology, Key Laboratory of Cell Differentiation and Apoptosis of Chinese Ministry of Education, Shanghai Jiao Tong University School of Medicine, Shanghai 200025, China

ARTICLE INFO

Keywords:
Leucine-rich repeat kinase 2 (LRRK2)
Acute kidney injury (AKI)
Chronic kidney disease (CKD)
Proximal tubular cell (PTC)
Mitochondrial damages
Mitofusin 2 (MFN2)

ABSTRACT

Mitochondrial dysfunction is one of the key features of acute kidney injury (AKI) and associated fibrosis. Leucine-rich repeat kinase 2 (LRRK2) is highly expressed in kidneys and regulates mitochondrial homeostasis. How it functions in AKI is unclear. Herein we reported that LRRK2 was dramatically downregulated in AKI kidneys. *Lrrk2*$^{-/-}$ mice exhibited less severity of AKI when compared to wild-type counterparts with less mitochondrial fragmentation and decreased reactive oxygen species (ROS) production in proximal renal tubular cells (PTCs) due to mitofusin 2 (MFN2) accumulation. Overexpression of *LRRK2* in human PTC cell lines promoted LRRK2-MKK4/JNK-dependent phosphorylation of MFN2^{Ser27} and subsequently ubiquitination-mediated MFN2 degradation, which in turn exaggerated mitochondrial damage upon ischemia/reperfusion (I/R) mimicry treatment. *Lrrk2* deficiency also alleviated AKI-to-chronic kidney disease (CKD) transition with less fibrosis. In vivo pre-treatment of LRRK2 inhibitors attenuated the severity of AKI as well as CKD, potentiating LRRK2 as a novel target to alleviate AKI and fibrosis.

1. Introduction

Acute kidney injury (AKI), characterized by rapid loss of kidney function, affects approximately 10–15% of patients admitted to the hospital among whom the prevalence can exceed 50% in the intensive care unit [1,2]. Despite the improvement in medical care, AKI remains high mortality approaching 50%–70% [3]. Moreover, AKI survivors bear approximately ~8.8-fold and ~3.1-fold increases in the risk to develop chronic kidney disease (CKD) and end-stage renal disease (ESRD) respectively [4], leading to great medical and economic burdens in the long run. Moreover, there is currently no definite therapy to prevent or treat established AKI per se.

Proximal tubular cells (PTCs) are responsible for the reabsorption of most nutrients existing in the glomerular ultrafiltrate [5]. PTCs located in S3 segment are extremely vulnerable to ischemia, toxic insults or mitochondrial damage related stimuli due to the high energy requirement and unique microvascular environment [6], mostly determining the severity of AKI. Impairment of PTC regeneration will prevent tissue repair, driving inflammation and fibrosis [7,8]. Therefore, maintaining PTC homeostasis is indispensable for AKI prevention and treatment.

* Corresponding authors. Department of Urology, Xinhua Hospital, School of Medicine, Shanghai Jiao Tong University, 1665 Kongjiang Road, Yangpu, Shanghai 200092, China.
** Corresponding author. Department of Urology, Xinhua Hospital, School of Medicine, Shanghai Jiao Tong University, 1665 Kongjiang Road, Yangpu, Shanghai 200092, China.
*** Corresponding authors. Department of Urology, Xinhua Hospital, School of Medicine, Shanghai Jiao Tong University, 1665 Kongjiang Road, Yangpu, Shanghai 200092, China.
**** Corresponding author. Shanghai Institute of Immunology, Department of Immunology and Microbiology, Shanghai Jiao Tong University School of Medicine, Shanghai 200025, China.
E-mail addresses: qiansubo@xinhuamed.com.cn (S. Qian), cuixingang@163.com (X. Cui), ywang@sibs.ac.cn (Y. Wang), shenhaibo@xinhuamed.com.cn (H. Shen).
[1] These authors contribute equally.

https://doi.org/10.1016/j.redox.2023.102860
Received 29 June 2023; Received in revised form 8 August 2023; Accepted 19 August 2023
Available online 22 August 2023

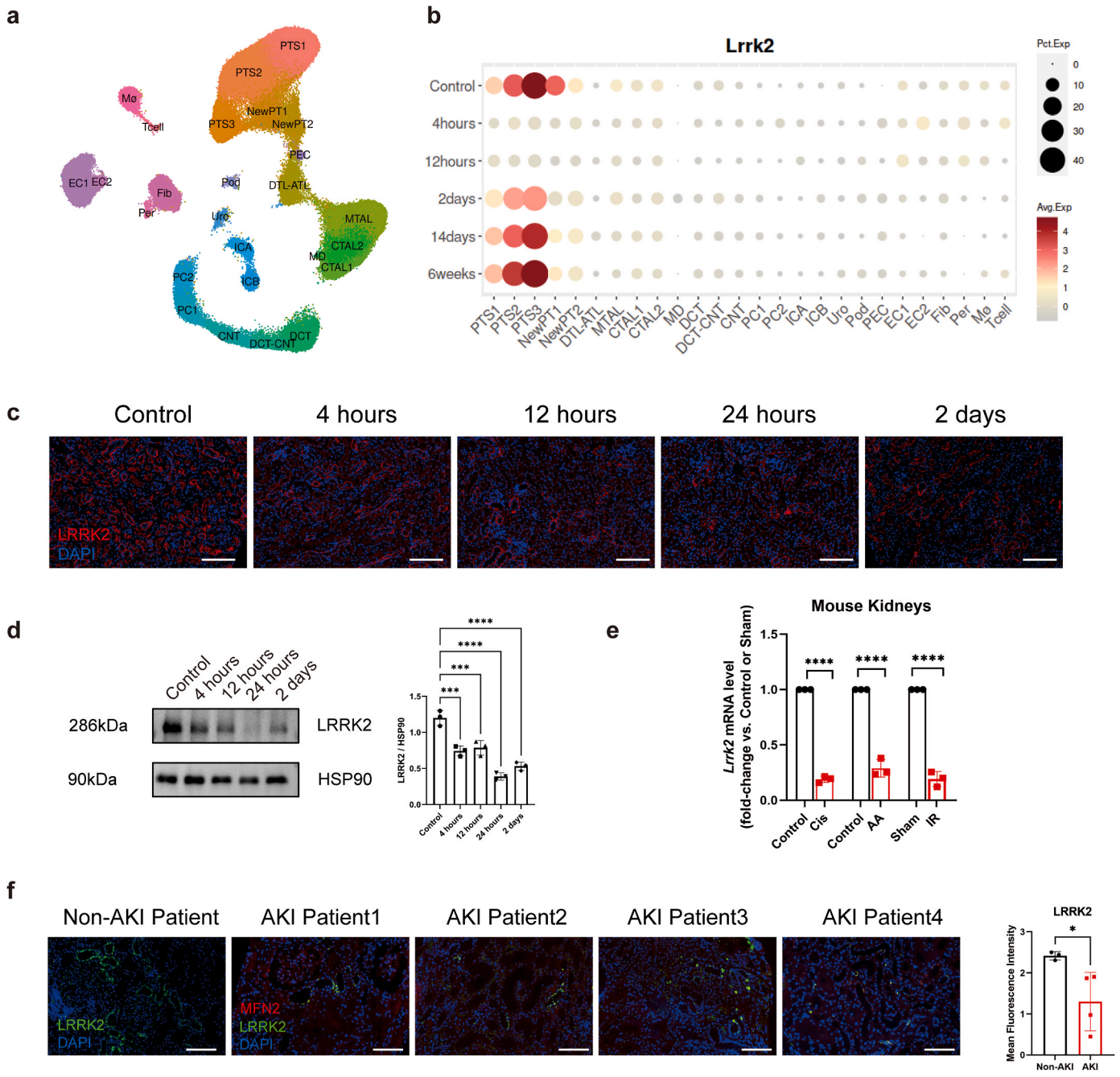

Fig. 1. *Lrrk2* expression decreased dramatically in acute phase of kidney injury

(a-b) UMAP plots (a) and gene expression analysis (b) of a scRNA-seq dataset from mice kidneys upon I/R at different time points.

(c) Representative images of LRRK2 immunostaining of the mouse kidneys upon I/R at different time points. Scale bar: 100 μm

(d) Immunoblotting analysis of LRRK2 in sham and I/R mouse kidneys upon I/R at different time points and quantification (n = 3/group).

(e) The mRNA level of *Lrrk2* in mouse kidneys after different ways of AKI induction (n = 3/group).

(f) Immunofluorescence staining of LRRK2 and MFN2 in human renal biopsy. Scale bar: 100 μm. The mean fluorescence intensity of LRRK2 was quantified.

Abbreviations UMAP Uniform Manifold Approximation and Projection, *scRNA-seq* single-cell RNA sequencing, *I/R* ischemia/reperfusion, *PT-S1* S1 segment of proximal tubule, *PT-S2* S2 segment of proximal tubule, *PT-S3* S3 segment of proximal tubule, *DTL* descending limb of loop of Henle, *ATL* thin ascending limb of loop of Henle, *MTAL* thick ascending limb of loop of Henle in medulla, *CTAL* thick ascending limb of loop of Henle in cortex, *MD* macula densa, *DCT* distal convoluted tubule, *CNT* connecting tubule, *ICA* type A intercalated cells of collecting duct, *ICB* type B intercalated cells of collecting duct, *Uro* urothelium, *Pod* podocytes, *PEC* parietal epithelial cells, *EC* endothelial cells, *Per* pericytes, *Fib* fibroblasts, *Mϕ* macrophages, *Cis* cisplatin, *AA* Aristolochic acid, *AKI* acute kidney injury

All the pooled data were presented as mean ± standard deviation (SD). The data were the representative of two independent experiments. A *Student's t*-test was used for statistical analysis between two groups. *p < 0.05, ***p < 0.001, ****p < 0.0001.

Mitochondria have been increasingly recognized as a critical player in AKI. PTCs need to generate a large amount of ATP via mitochondrial oxidative phosphorylation due to high-energy demand to fulfill their reabsorption function [9]. Being the powerhouse of the cells, one of the mechanisms for the mitochondria in response to functional adaptation and the requirement for energy is highly dynamic that constantly undergoes fusion and fission transformation. Mitochondria fusion is a process where two mitochondria merge their membranes to form a

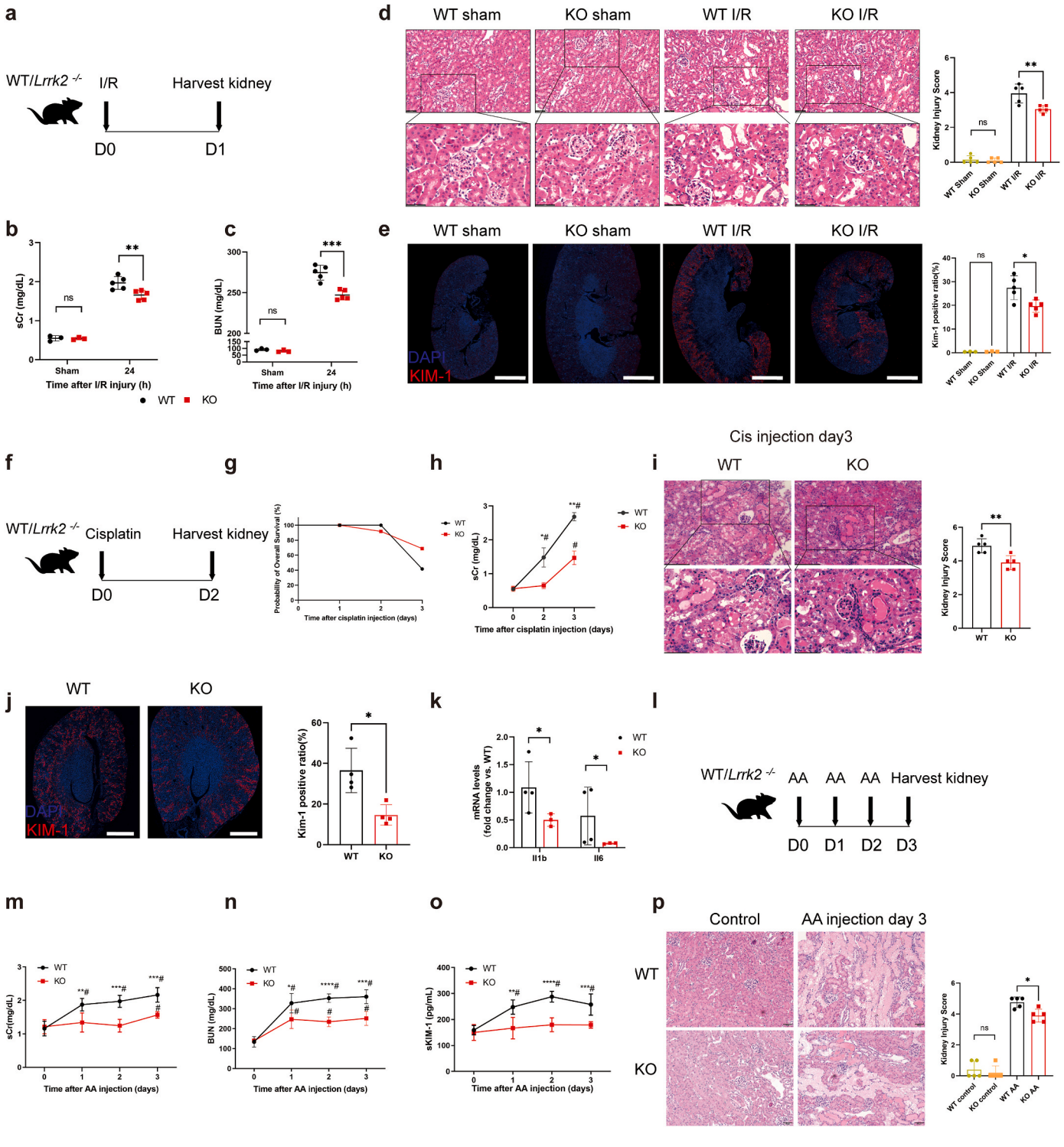

(caption on next page)

Fig. 2. *Lrrk2*$^{-/-}$ mice display less severity of acute kidney injury than WT mice.
(a) Experimental scheme of I/R-induced AKI model.
(b–c) Comparison of sCr (c) and BUN (d) between WT and *Lrrk2*$^{-/-}$ mice 24 h after I/R injury (n = 5/group).
(d) Representative image of H&E staining of the kidneys (left) and quantification of the tubulointerstitial damage (n = 10 fields/section) 24 h after I/R injury (right). Scale bar: 50 μm
(e) Representative images of KIM-1 immunostaining of the kidneys (left) and quantification of the Kim-1 positive ratio 24 h after I/R injury (right). Scale bar: 50 μm
(f) Experimental scheme of cisplatin-induced AKI model.
(g) Mortality rates after cisplatin injection in WT and *Lrrk2*$^{-/-}$ mice (n = 12/group).
(h) Comparison of dynamic sCr levels in WT and *Lrrk2*$^{-/-}$ mice after cisplatin injection (n = 5/group).
(i) Representative images of H&E staining of the kidneys (left) and quantification of the tubulointerstitial damage (right) (n = 10 fields/section) 3 days after cisplatin injection. Scale bar: 50 μm
(j) Representative images of KIM-1 immunostaining of the kidneys (left) and quantification of KIM-1 positive ratio (right) 3 days after cisplatin injection. Scale bar: 50 μm
(k) Comparisons of *Il1b* and *Il6* mRNA levels (fold change *vs.* one replicate in WT group) in cisplatin-injured kidneys from WT and *Lrrk2*$^{-/-}$ mice (n = 4/group).
(l) Experimental scheme of AA-induced AKI model.
(m-o) Comparisons of dynamic sCr (m), BUN (n), and serum KIM-1 (o) in WT and *Lrrk2*$^{-/-}$ mice after AA injury (n = 5/group).
(p) Representative images of H&E staining of the kidneys (left) and quantification of the tubulointerstitial damage (right) (n = 10 fields/section) 3 days after AA injury. Scale bar: 50 μm.
Abbreviations sCr serum creatinine, *BUN* blood urea nitrogen, *WT* wild type, *KO Lrrk2* knockout, *I/R* ischemia/reperfusion, *KIM-1* kidney injury molecule-1, *Cis* cisplatin, *AA* Aristolochic acid
All the pooled data were presented as mean ± standard deviation (SD). The data were representative of two independent experiments. A *Student's t*-test was used for statistical analysis between two groups. *p < 0.05,**p < 0.01,***p < 0.001, ****p < 0.0001 vs. KO, #p < 0.05 *vs.* D0, ns: no significance.

larger mitochondrion which is mainly mediated by Mitofusin 1/2 (MFN1/2). Fission is the opposite process where a mitochondrion divides into two daughter organelles, which is mainly mediated by dynamin-related protein 1 (DRP1) [10]. The balance between fusion and fission is very important for mitochondria function. Unopposed mitochondrial dynamics could lead to abnormal generation of ATP [11], extra production of mitochondrial reactive oxygen species (mtROS) [12], release of cytochrome *c* [13], leakage of mitochondrial DNA (mtDNA) into the cytosol [14], and ultimately cell death which dedicates to aggravated AKI. It also gives rise to renal microvascular damage and fibrosis, which are the most important pathogenic factors for CKD progression after AKI [15,16]. Therefore, maintaining mitochondria integrity and function in PTCs is beneficial for the outcome of the injured kidney.

Leucine-rich repeat kinase 2 (LRRK2) is a protein containing multiple functional domains including ankyrin repeat region, leucine-rich repeat (LRR) domain, ROC (Ras of complex proteins) GTPase domain, *C*-terminal of ROC (COR) domain, kinase domain related to mitogen-activated protein kinase kinase kinase (MAPKKK) and *C*-terminal WD40 region [17]. It is highly expressed in various tissues including the kidney, lung, brain, and certain immune cells [18]. Mutations of *LRRK2* have emerged as closely associated with Parkinson's disease (PD) [19] and some immune-related disorders [20–22] where the underlying mechanism is still ambiguous. Recent studies have gradually elucidated the modes of LRRK2 in regulating mitochondrial homeostasis. In PD patients, *LRRK2*^{G2019S} mutation enhances RAB10 phosphorylation, resulting in the accumulation of RAB10 and autophagy receptor optineurin on depolarized mitochondria and the impairment of mitophagy [23]. In *LRRK2*^{R1441G} mutant Parkinsonian mice, aberrant mitochondrial morphology and function are companied by impaired mitophagy and the activation of DRP1-MAPK/ERK signaling pathway [24]. Dysfunction of LRRK2 has been demonstrated to be involved in lung fibrosis [25,26], heart remodeling [27], kidney function [28–30], *etc*. Previously, we have reported that LRRK2 deficiency attenuated pristane-induced lupus-like pathology and renal injury in mice [33]. However, how LRRK2 regulates mitochondrial function during AKI pathogenesis remains unclear.

In this study, we report that LRRK2 is highly expressed in PTCs and markedly downregulated during kidney injury. *Lrrk2*$^{-/-}$ mice display less severity of kidney injury in the model of AKI, characterized by reduction of mitochondrial fragmentation and ROS production in PTCs. These defects are aggravated by LRRK2 overexpression. Mechanistically, LRRK2 indirectly phosphorylates MFN2 via the MKK4-JNK pathway, leading to ubiquitination-mediated MFN2 degradation. MFN2 reduction causes mitochondrial damage and ROS accumulation, contributing to the cell death of PTCs and aggravation of kidney injury. Furthermore, LRRK2 deficiency alleviates chronic kidney fibrosis. Finally, pretreatment of LRRK2 inhibitors attenuated the severity of AKI and chronic kidney fibrosis *in vivo*. Therefore, LRRK2 downregulation represents an important mechanism to prevent mitochondrial dysfunction and protect AKI and chronic kidney fibrosis, suggesting LRRK2 inhibition as a novel strategy for these diseases.

1.1. Methods

1.1.1. Mice

Lrrk2$^{-/-}$ mice (*Lrrk2*$^{-/-}$ C57BL/6N-Lrrk2tm1.Mjff/J; approved by the Michael J. Fox Foundation for Parkinson's research; JAX stock 016121) were purchased from the Jackson Laboratory (USA). Age- and gender-matched WT mice were used as controls in all experiments. All mice were maintained in individually ventilated cages under specific pathogen-free (SPF) conditions in the animal facility of Shanghai Jiao Tong University School of Medicine.

1.1.2. Animal models

Male mice between 8 and 12 weeks old were used in the induction of kidney injury. An ischemia/reperfusion (I/R) AKI mouse model was induced by ischemia for 30 min at 37 °C in the left kidney using the flank approach as previously reported and contralateral nephrectomy [31]. Alternatively, cisplatin toxic AKI mouse model was induced by intraperitoneal injection of cisplatin (P4394, Merck) in 0.9% saline (20 mg/kg) [32], and Aristolochic acid (AA) toxic AKI mouse model was induced by intraperitoneal injection of AA (A5512, Merck) (10 mg/kg) for 3 consecutive days [33]. Three AKI-CKD mice models were generated in this study. I/R AKI-CKD mice were induced by ischemia for 45 min at 37 °C in the left kidney while the right kidney was preserved for 2 weeks [34]. Cisplatin-induced AKI-CKD model was generated by repeated injection of low-dose cisplatin (10 mg/kg) once weekly for four times [35]. UUO (unilateral ureteral obstruction) AKI-CKD mouse model was established by complete obstruction of the left ureter for 7 days [36].

1.1.3. In vitro I/R mimicry treatment

For imitating I/R injury *in vitro*, HK-2 cells were induced by changing the culture medium to serum/glucose-free medium containing 10 μM CCCP (HY-100941, MedChemExpress). After 4 h, the medium was replaced with fresh culture medium containing serum and glucose for 2 h.

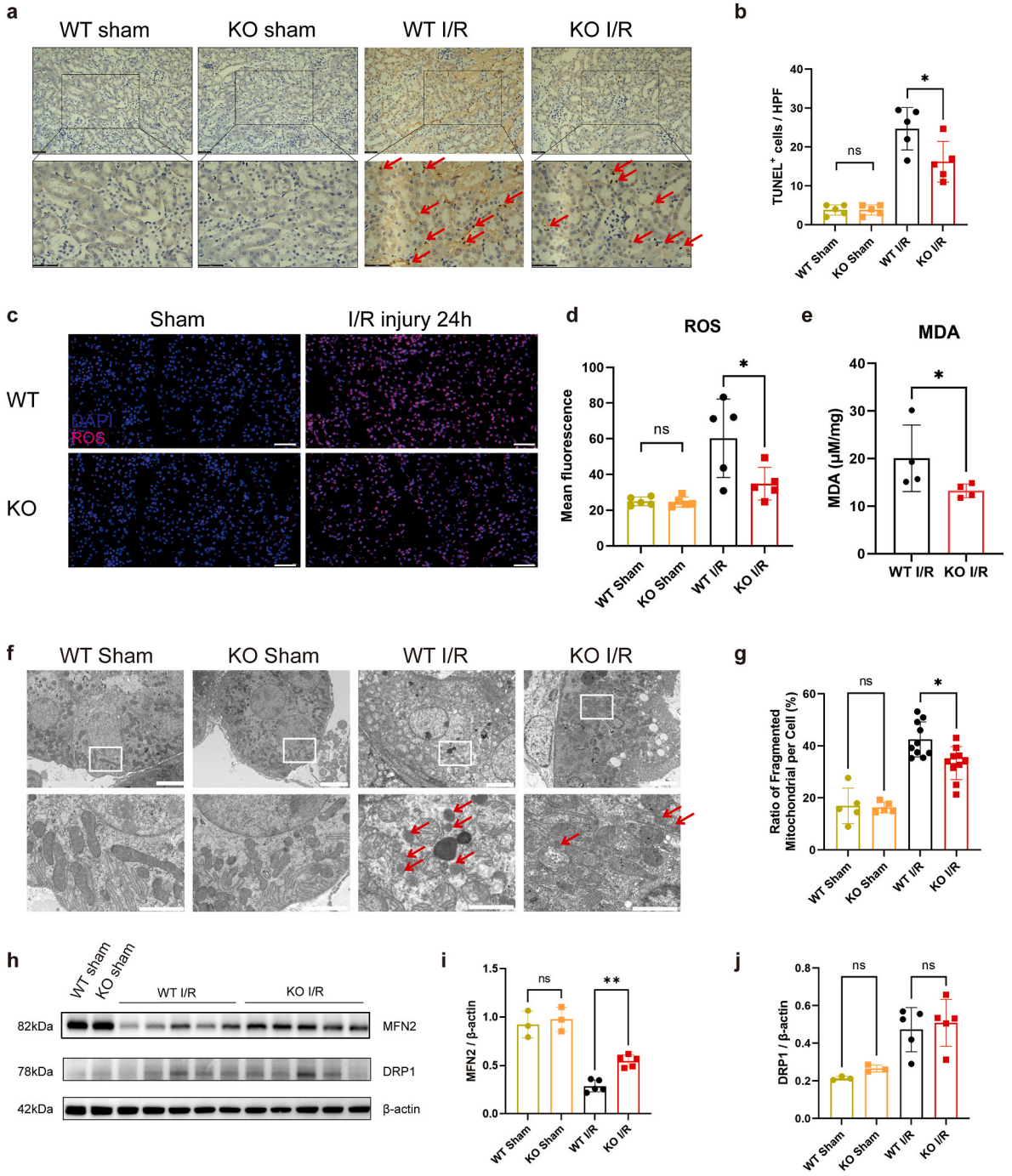

Fig. 3. *Lrrk2*$^{-/-}$ AKI mice exhibit less mitochondrial injury together with increased MFN2 protein levels in the kidneys.
(**a-b**) Representative of TUNEL staining of the kidneys from WT and *Lrrk2*$^{-/-}$ mice (a) and quantification of TUNEL^{+} cells (b) (n = 5 fields/section) at 24 h after I/R injury. Red arrows showed the TUNEL^{+} cells. Scale bar: 50 μm
(**c-d**) DHE staining (c) and quantification (d) of ROS production in the kidneys from WT and *Lrrk2*$^{-/-}$ mice (n = 5 fields/section) at 24 h after I/R injury. Scale bar: 50 μm
(**e**) Comparison of MDA levels in the kidneys from WT and *Lrrk2*$^{-/-}$ mice at 24 h after I/R injury.
(**f-g**) Transmission electron microscope assay of the kidneys from WT and *Lrrk2*$^{-/-}$ mice at 24 h after I/R injury (n = 3/group). Normal Mitochondria were intact and approximately 1–3 μm in length. The red arrows showed fragmented mitochondria which appeared shorter lengths of <0.5 μm (f). Scale bar: 5 μm (up), 2 μm (down). Raito of fragmented mitochondria per cell was quantified in individual cells (n = 5 cells in sham group and n = 10 cells in I/R group) (g).
(**h-j**) Detection (h) and quantification of MFN2 (i) and DRP1 (j) expression in WT and *Lrrk2*$^{-/-}$ kidneys at 24 h after I/R injury by Western blot.
Abbreviations WT wild-type, *KO* knockout, *I/R* ischemia/reperfusion, *ROS* reactive oxygen species, *MDA* malonic dialdehyde, *MFN2* mitofusin 2, *DRP1* dynamin-related protein 1
All the pooled data were presented as mean ± SD. The data were representative of two independent experiments. A *Student's t*-test was used for statistical analysis between two groups. Ns: no significance, *p < 0.05,**p < 0.01. (For interpretation of the references to colour in this figure legend, the reader is referred to the Web version of this article.)

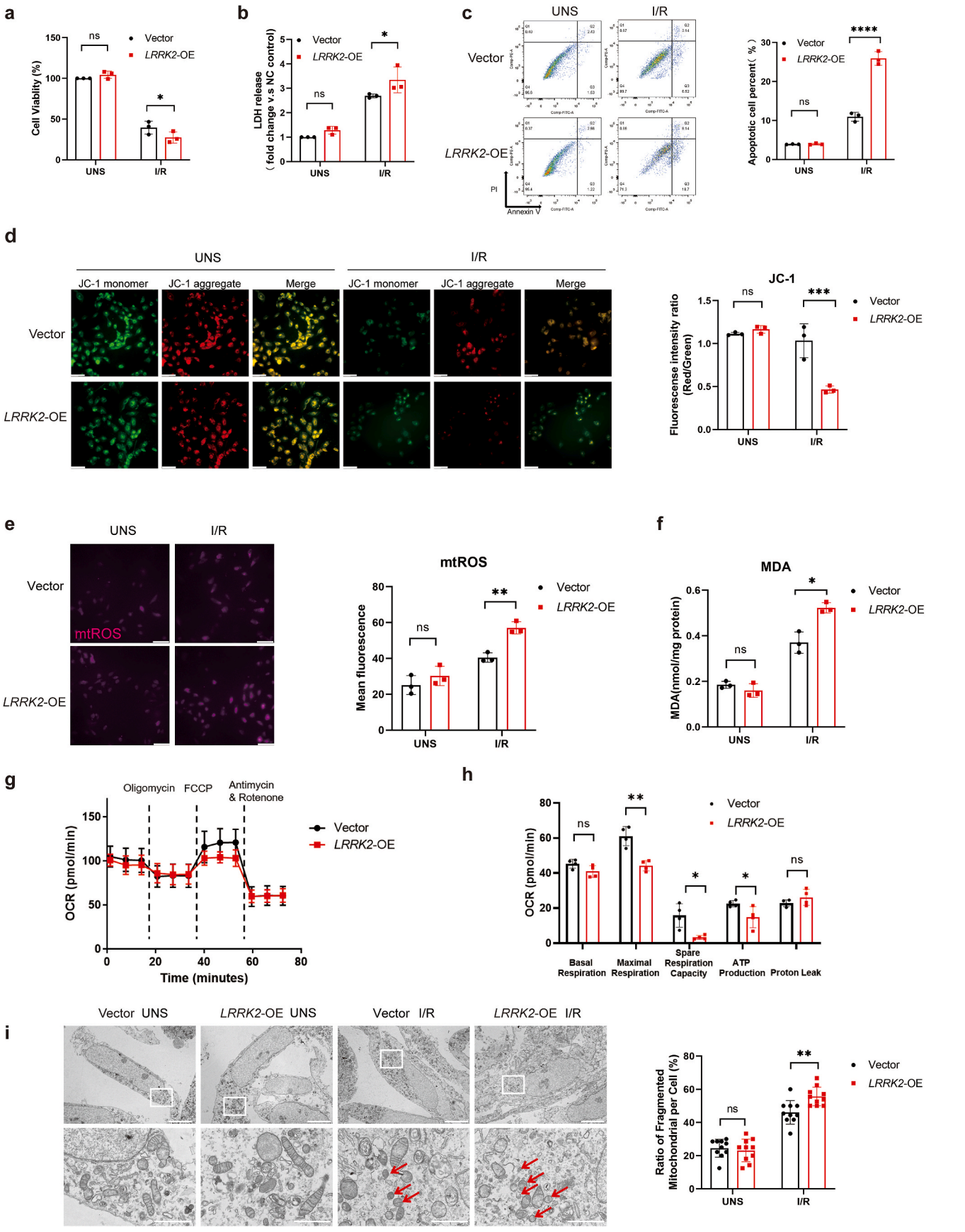

(caption on next page)

Fig. 4. *LRRK2* overexpression in HK-2 cells aggravates cell injury with mitochondrial defects after *in vitro* I/R mimicry treatment.
HK-2 cells were transiently transfected with 2xMyc-*LRRK2*-WT and control vector for 48 h. Cells were subjected to the induction of I/R by changing the medium to serum/glucose-free medium containing 10 μM CCCP to mimic the ischemia condition *in vivo*. After 4 h, the medium was replaced with fresh medium containing serum and glucose for 2 h to mimic the reperfusion *in vivo*.
(**a**) Cell viability of HK-2-Vector and HK-2-*LRRK2*-OE cells by the CCK-8 assay. Cell viability was normalized to HK-2-Vector without treatment (UNS group) (n = 3/group). (**b**) LDH release assay on HK-2-Vector and HK-2-*LRRK2*-OE cells. LDH release level was normalized to HK-2-Vector without treatment (UNS group) (n = 3/group).
(**c**) Detection (left) and quantitative analysis (right) of apoptotic HK-2 Vector and HK-2-*LRRK2*-OE cells by Annexin V-PI analysis (n = 3/group).
(**d**) Detection (left) and quantitative analysis (right) of mitochondrial transmembrane potential of HK-2-Vector and HK-2-*LRRK2*-OE cells by JC-1 staining (n = 3/group). Scale bar: 100 μm
(**e**) Representative images of mtROS staining (left) in HK-2-Vector and HK-2-*LRRK2*-OE cells (n = 3/group) and quantification (right). Scale bar: 100 μm
(**f**) MDA detection in HK-2-Vector and HK-2-*LRRK2*-OE cells (n = 3/group).
(**g-h**) OCR influxes of HK-2-Vector cells versus HK-2-*LRRK2* cells detected by Seahorse (n = 4/group).
(**i**) Transmission electron microscope assay of HK-2-Vector and HK-2-*LRRK2*-OE cells (left). Red arrows showed fragmented mitochondria. Scale bar: 10 μm (up), 1 μm (down). Fragmented mitochondria were counted in 10 cells/group and compared between HK-2-Vector and HK-2-*LRRK2*-OE cells (right).
Abbreviations WT wild-type, *OE* overexpression, *UNS* unstimulated, *LDH* lactate dehydrogenase, *mtROS* mitochondrial reactive oxygen species, *MDA* malonic dialdehyde, *OCR* oxygen consumption rate.
All the pooled data were presented as mean ± SD. The data were representative of three independent experiments. A *Student's t*-test was used for statistical analysis between two groups. Ns no significance, *p < 0.05,**p < 0.01, ***p < 0.001, ****p < 0.0001. (For interpretation of the references to colour in this figure legend, the reader is referred to the Web version of this article.)

1.1.4. Statistical analysis

Data were presented by mean ± standard deviation (SD). Statistical comparisons were performed using the statistical software GraphPad Prism 9 (GraphPad Software, San Diego, CA, USA). The differences between two groups were tested using a *Student's t*-test. The intergroup differences among three or more groups were tested using one-way analysis of variance (ANOVA).

Details for the rest methods are given in the Supplementary Methods.

2. Results

2.1. Lrrk2 expression is dramatically decreased in acute phase of kidney injury

To find out the role of LRRK2 in AKI, we analyzed single-cell RNA sequencing data from mouse I/R-induced kidneys at different time points [37] (Fig. 1a). It was found that *Lrrk2* was mainly expressed in normal PTCs including PTS1-PTS3 cells (Fig. 1b). However, we observed a quick down-regulation of *Lrrk2* gene in acute phase of I/R injury and a restoration after 2 days (Fig. 1b). Results from immunostaining and immunoblot also proved the changes of LRRK2 protein in tubular cells in mouse renal cortex along with the induction time of I/R, but the change rate at protein level was slower than at mRNA level (Fig. 1c–d). Consistently, in other AKI mice models including cisplatin and aristolochic acid (AA) models, the mRNA levels of *Lrrk2* in the kidneys also showed dramatic decreases as compared to control kidneys (Fig. 1e). In addition, in human AKI renal biopsy specimens, we observed much lower expressions of LRRK2 compared to non-AKI patients (Fig. 1f). These results suggest that LRRK2 may play an important role in kidney injury.

2.2. Lrrk2 deficiency leads to less severity of AKI in mice

We thereafter used *Lrrk2*$^{-/-}$ mice (Figs. S1a–b) to determine the role of LRRK2 during AKI. AKI was induced in WT and *Lrrk2*$^{-/-}$ mice by I/R injury (Fig. 2a). It was apparent that there exhibited lower levels of sCr and BUN (Fig. 2b–c) in *Lrrk2*$^{-/-}$ mice. Consistently, we found less tubular necrosis, cast formation, and tubular dilation in the kidneys from *Lrrk2*$^{-/-}$ mice, which was represented by the kidney injury score (Fig. 2d). Kidney injury molecule-1 (KIM-1) is a biomarker of kidney injury [38]. KIM-1^{+} cell numbers were lower in *Lrrk2*$^{-/-}$ kidneys than those in WT kidneys (Fig. 2e) as well.

AKI was also induced by cisplatin (Fig. 2f) where WT mice showed higher mortality than *Lrrk2*$^{-/-}$ mice within 3 days after cisplatin injection (Fig. 2g). WT mice showed higher sCr levels 2 and 3 days after cisplatin injection (Fig. 2h). At day 3, kidney injury score (Fig. 2i) and KIM-1^{+} cell number (Fig. 2j) were also lower in *Lrrk2*$^{-/-}$ kidneys than those in WT kidneys. Consistently, mRNA levels of key proinflammatory cytokines including *Il1b* and *Il6* were less detectable in *Lrrk2*$^{-/-}$ kidneys (Fig. 2k).

We also validated the protection of *Lrrk2* deficiency in the AA-induced AKI model (Fig. 2l). Similarly, both sCr and BUN (Fig. 2m-n) levels were dramatically lower in *Lrrk2*$^{-/-}$ mice. The concentrations of serum KIM-1 were significantly lower in *Lrrk2*$^{-/-}$ mice (Fig. 2o) together with less kidney damage (Fig. 2p). Although it was reported that there were age-dependent alterations in the kidneys of *Lrrk2*$^{-/-}$ mice [29], there showed no dramatic difference in sCr and BUN levels between 3-month and 6-month-old mice in cisplatin-induced AKI models (Figs. S1c–d). Based on the data from three AKI mice models, it is well supported that *Lrrk2* deficiency protects the mice from AKI with less severity.

2.3. Lrrk2 deficiency in immune cells does not dedicate to the alleviation of kidney injury in Lrrk2$^{-/-}$ mice

Infiltration and function impairment of immune cells, especially the macrophages, are key features during pathogenic injury and tissue repair after AKI [39,40]. Since LRRK2 is also abundant in specific immune cells including monocytes and macrophages [41,42], we tested whether *Lrrk2* in immune cells played a role in AKI. Flow cytometric analysis revealed no difference in the numbers of macrophages, Ly6C^{hi} monocytes, and Ly6C^{low} monocytes as well as other immune cells in the kidneys between WT and *Lrrk2*$^{-/-}$ mice in the I/R AKI model (Figs. S2a–f, S3a-c). In addition, upon *in vitro* stimulation of lipopolysaccharide (LPS) and Pam3CSK4, there displayed no difference in the expressions of *Tnf, Il6,* and *Il1b* (Figs. S3d–f) by BMDMs from WT and *Lrrk2*$^{-/-}$ mice. When stimulated with M-CSF and IL-4 *in vitro*, the hallmarks of alternatively activated macrophages such as Arg*1* and *Chil3* (Figs. S3g–h) also showed no difference. The expressions of CD86 (a biomarker of classically activated macrophages) and CD206 (a biomarker of alternatively activated macrophages) on BMDMs upon stimulation were also comparable (Fig. S3i). Inflammatory cytokines like TNF-α and IL-6 (Figs. S3j–k) were also at similar levels in the culture supernatants of BMDMs from WT and *Lrrk2*$^{-/-}$ mice upon LPS stimulation.

We further generated bone marrow (BM) chimeric mice by transferring BM cells either from WT and *Lrrk2*$^{-/-}$ mice to irradiated *Lrrk2*$^{-/-}$ mice (Fig. S3l). The levels of sCr and BUN (Fig. S3m-n) were similar between BM-WT and BM-*Lrrk2*$^{-/-}$ transferred mice after AKI induction, together with no obvious difference in kidney damage and KIM-1 expression (Fig. S3o-p). These data demonstrate that *Lrrk2* deficiency in immune cells does not dedicate to the alleviation of experimental AKI

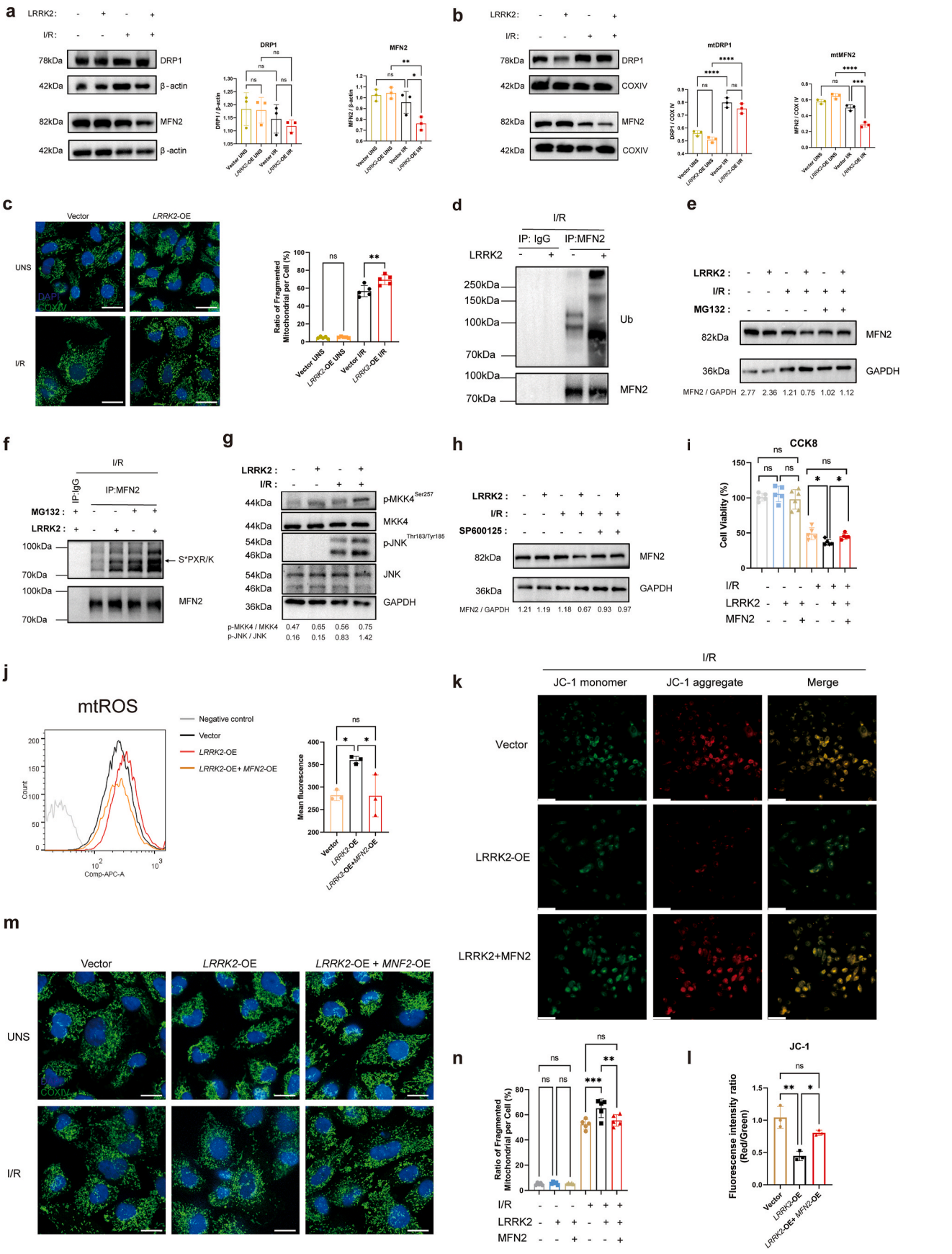

(caption on next page)

Fig. 5. LRRK2 promotes ubiquitination-mediated MFN2 degradation in the MKK4/JNK-dependent pathway in response to I/R mimicry treatment.
(**a-b**) Immunoblot analysis and quantification of MFN2 and DRP1 in whole cell lysate (WCL) (a) and isolated mitochondria (b) in HK-2-Vector and HK-2-*LRRK2*-OE cells upon I/R mimicry treatment. β-Actin was used as WCL loading control. COX IV was used as the mitochondrial loading control.
(**c**) Mitochondrial morphology was evaluated by immunostaining of mitochondrial protein COX IV. Mitochondrial of untreated cells were filamentous, while mitochondrial in stressed cells were fragmented and appeared shortened and punctate. The ratios of fragmented mitochondria were quantified in individual cells (right). Scale bar: 20 μm
(**d**) Detection of ubiquitination of MFN2 after immunoprecipitation with an anti-MFN2 antibody through immunoblotting with antibodies recognizing ubiquitin or MFN2.
(**e**) Expression levels of MFN2 in whole-cell lysates of HK-2-Vector and HK-2-*LRRK2*-OE cells upon I/R mimicry treatment *in vitro* with or without MG132 (20 μM) for 2 h. The data were representative of three independent experiments.
(**f**) Immunoprecipitated endogenous MFN2 in HK-2-Vector and HK-2-*LRRK2*-OE cells upon I/R mimicry treatment was immunoblotted with antibodies recognizing either S*PXR/K (S* = phospho-serine) or MFN2.
(**g**) Whole-cell lysates of HK-2-Vector and HK-2-*LRRK2*-OE cells were immunoblotted with antibodies recognizing JNK/p-JNK$^{Thr183/Tyr185}$ and MKK4/p-MKK4^{Ser257}. The data were representative of three independent experiments.
(**h**) HK-2-Vector and HK-2-*LRRK2*-OE cells were treated with or without JNK inhibitor SP600125 (20 μM) 2 h prior to I/R mimicry treatment. Whole-cell lysates were immunoblotted with an antibody recognizing MFN2. The data were representative of three independent experiments.
(**i-j**) HK-2 cells were transfected with 2xMyc-*LRRK2* or co-transfected with 2xMyc-*LRRK2*-WT and *MFN2*, and subjected to I/R mimicry treatment. Cell viability was detected by CCK8 assay (n = 3/group) (i) and mtROS was detected by mtSOX Deep Red staining (j, left) and quantified by fluorescence intensity was detected (j, right) (n = 3/group).
(**k-l**) Detection of the mitochondrial transmembrane potential of the cells by JC-1 staining (n = 3/group) in HK-2-*LRRK2*-OE and HK-2-*LRRK2*-OE-*MFN2* cells. Scale bar: 100 μm
(**m-n**) Mitochondrial morphology was evaluated by immunostaining of mitochondrial protein COX IV (m). The ratios of fragmented mitochondria were quantified in individual cells (n). Scale bar: 20 μm.
Abbreviations I/R ischemia/reperfusion, *IP* immunoprecipitation, *OE* overexpression, *UNS* unstimulated, *mtROS* mitochondrial reactive oxygen species, *DRP1* dynamin-related protein 1, *MFN2* mitofusin2, *Ub* ubiquitin
All the pooled data were presented as mean ± SD. One-way ANOVA was used for statistical analysis among the different groups. Ns no significance, ns no significance, *p < 0.05,**p < 0.01, ***p < 0.001, ****p < 0.0001. (For interpretation of the references to colour in this figure legend, the reader is referred to the Web version of this article.)

pathogenesis.

2.4. *Lrrk2*$^{-/-}$ AKI mice exhibit less mitochondrial injury together with increased MFN2 protein levels in the kidneys

We further determined whether LRRK2 modulated the fate of PTCs upon I/R. TUNEL $^{+}$ cells were less detectable in the kidneys of *Lrrk2*$^{-/-}$ mice, suggesting less apoptosis of PTCs (Fig. 3a–b). LRRK2 has been demonstrated to be involved in mitochondrial homeostasis [23], which is one of the key causes of death of PTCs during AKI. We noticed that less ROS was generated in the kidneys from *Lrrk2*$^{-/-}$mice after I/R (Fig. 3c–d). Consistently, the end product of lipid peroxidation malonic dialdehyde (MDA) levels were lower in the kidneys of *Lrrk2*$^{-/-}$mice (Fig. 3e). By TEM, we observed no difference of mitochondrial morphology in the uninjured *Lrrk2*$^{-/-}$ and WT mice kidneys, but there existed more fragmented mitochondria in PTCs from WT mice after I/R (Fig. 3f–g). We further detected the expression of MFN2 and DRP1, the most relevant proteins engaged in fusion and fission, respectively [43]. *Lrrk2* deficiency partially restored MFN2 levels of the kidneys after I/R when compared to WT mice (Fig. 3h–i). Consistently, in human kidney biopsy specimens, we observed lower MFN2 expression where LRRK2 expression was higher (Fig. 1f). On the contrary, no difference was found between *Lrrk2*$^{-/-}$ and WT mice (Fig. 3j). Our data from *in vivo* AKI mouse model demonstrate that *Lrrk2* deficiency alleviates mitochondrial injury accompanied by the alteration of MFN2 levels after kidney injury.

2.5. LRRK2 overexpression in HK-2 cells aggravates cell injury with mitochondrial defect after in vitro I/R mimicry treatment

To investigate how LRRK2 modulated the function of renal tubular cells during AKI, we overexpressed *LRRK2* in human kidney PTC cell line HK-2 cells (HK-2-*LRRK2*) whose LRRK2 expression was dramatically low (Fig. S4). Then HK-2-*LRRK2* and HK-2-Vector cells were treated with I/R *in vitro* [44]. HK-2-*LRRK2* cells showed less cell viability after *in vitro* I/R mimicry treatment (Fig. 4a). LDH release was more dramatic by HK-2-*LRRK2* cells (Fig. 4b). More apoptotic cells were detected in HK-2-*LRRK2* cells than in HK-2-Vector cells (Fig. 4c). These results indicated that LRRK2 overexpression led to more cell death upon I/R injury.

We further detected the effects of LRRK2 overexpression on mitochondrial homeostasis. JC-1 is a widely-used probe for the assessment of mitochondrial membrane potential. At higher potentials, JC-1 aggregates accumulate within mitochondria and form red fluorescent. When the membrane potential is low, it exists as a monomer and forms green fluorescent. It was apparent that HK-2-*LRRK2* cells exhibited fewer JC-1 aggregates in the cytosol, indicating the loss of mitochondrial membrane potential to more extent (Fig. 4d). On the contrary, mtROS induction and MDA levels were much higher in HK-2-*LRRK2* cells (Fig. 4e–f). HK-2-*LRRK2* cells also showed significantly lower mitochondrial oxygen consumption rate (OCR) with lower mitochondrial spare respiratory capacity and ATP production than HK-2-Vector cells (Fig. 4g–h). However, no difference of extracellular acidification rate (ECAR) was found in HK-2-*LRRK2* cells when compared with HK-2-Vector cells (Figs. S5a–b). Results from TEM analysis showed that there were more fragmented mitochondria in HK-2-*LRRK2* cells after I/R (Fig. 4i). These results indicate that overexpression of LRRK2 in PTC cells causes more cell death upon I/R accompanied by mitochondrial injury.

2.6. LRRK2 promotes ubiquitination-mediated MFN2 degradation through MKK4/JNK-dependent pathway in response to I/R treatment

ROS levels are well regulated by the mitochondrial antioxidant defense system consisting of antioxidant enzymes including superoxidase dismutases (SODs) and glutathione peroxidases (GSH-Px) [9]. Although the levels of mtROS and MDA (Fig. 4e–f) were higher in HK-2-*LRRK2* cells, the activity of GSH-Px, T-SOD, and CuZn-SOD were comparable between HK-2-*LRRK2* and control cells (Figs. S6a–c). Therefore, we further detected the influence of fusion and fission. We found that DRP1 showed no difference between HK-2-*LRRK2* and HK-2-Vector cells. However, both cytosolic and mitochondrial MFN2 levels were down-regulated with more extent in HK-2-*LRRK2* cells, which was in accordance with *in vivo* I/R results from *Lrrk2*$^{-/-}$ mice (Fig. 5a–b). To visualize the influence of mitochondrial fusion, we further detected mitochondrial integrity through immunostaining of a mitochondrial protein COXIV. It was apparent that more fragmented mitochondria were detected in HK-2-*LRRK2* cells after I/R (Fig. 5c). These results

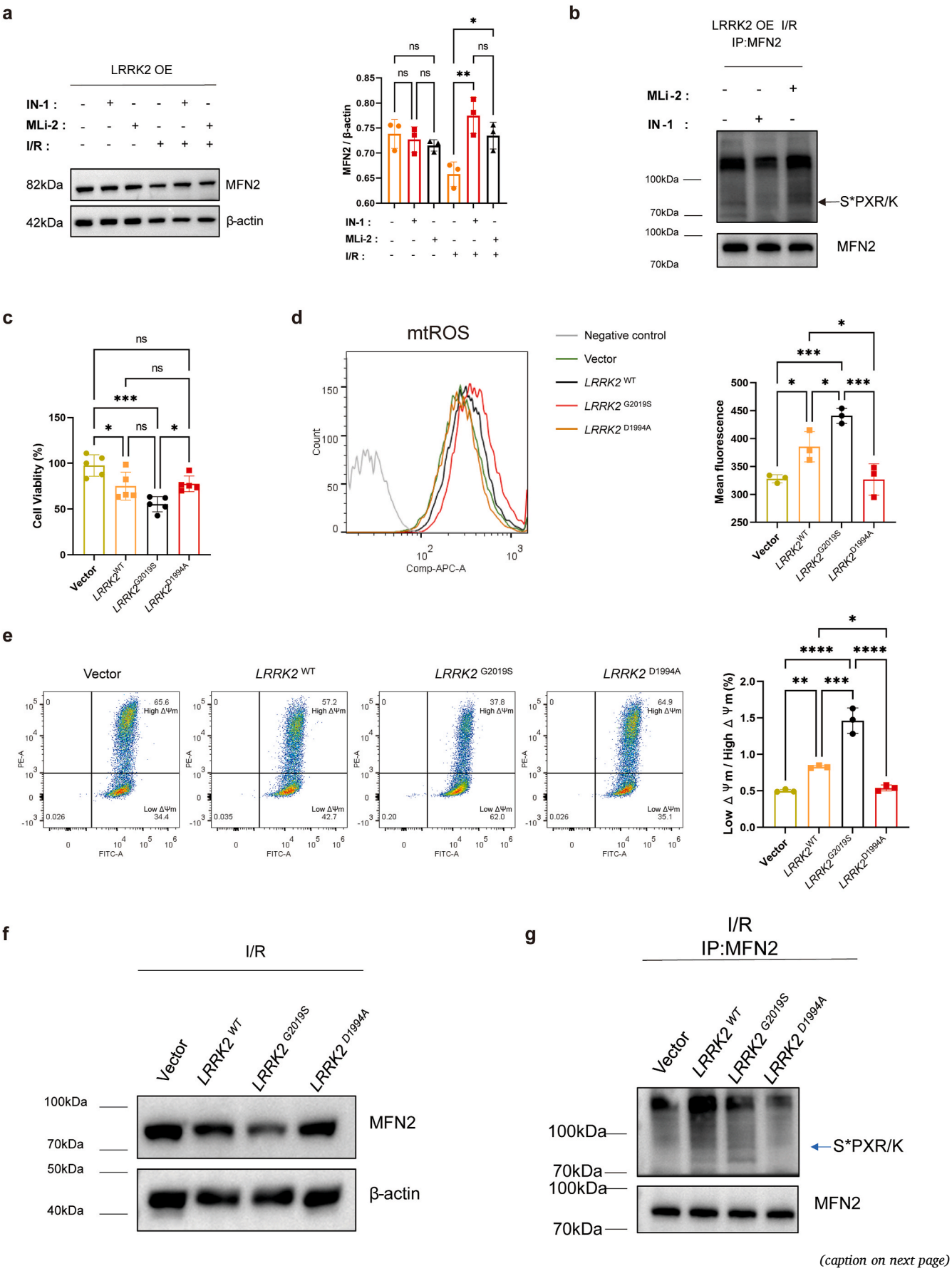

(caption on next page)

Fig. 6. LRRK2 kinase activity promotes the apoptosis of HK-2 cells with decreased MFN2 levels and more mitochondrial injury exposed to *in vitro* I/R treatment.
(**a**) MFN2 expression in HK-2-*LRRK2*-OE cells treated with LRRK2-IN-1 (1 μM) or MLi-2 (1 μM) 2 h prior to being induced by I/R *in vitro* by immunoblotting.
(**b**) Immunoprecipitated endogenous MFN2 from HK-2-*LRRK2*-OE cells was immunoblotted with the antibodies recognizing either S*PXR/K or MFN2. c-g HK-2 cells transfected with Vector, 2xMyc-$LRRK2^{WT}$, 2xMyc-$LRRK2^{G2019S}$, or 2xMyc-$LRRK2^{D1994A}$ were induced by I/R *in vitro*.
(**c-d**) Comparisons of cell viability (c) and mtROS (d) levels among HK-2-$LRRK2^{WT}$, HK-2-$LRRK2^{G2019S,}$ and HK-2-$LRRK2^{D1994A}$ cells. The cell viability(%) was normalized to one replicate in HK-2-Vector group.
(**e**) Detection (left) and quantification (right) of mitochondrial transmembrane potential of HK-2-$LRRK2^{WT}$, HK-2-$LRRK2^{G2019S}$, and HK-2-$LRRK2^{D1994A}$ cells by flow cytometry.
(**f**) Detection of MFN2 levels in HK-2-Vector, HK-2-$LRRK2^{WT}$, HK-2-$LRRK2^{G2019S}$ and HK-2-$LRRK2^{D1994A}$ cells upon I/R mimicry treatment.
(**g**) Immunoprecipitated endogenous MFN2 from HK-2-Vector, HK-2-$LRRK2^{WT}$, HK-2-$LRRK2^{G2019S}$ and HK-2-$LRRK2^{D1994A}$ cells were immunoblotted with antibodies recognizing either S*PXR/K (S* = phospho-serine) or MFN2.
Abbreviations WT wild-type, OE overexpression, *IP* immunoprecipitation, *mtROS* mitochondrial reactive oxygen species, $\Delta\Psi m$ mitochondrial transmembrane potential, *I/R* ischemia/reperfusion
All the pooled data were presented as mean ± SD. The data were representative of three independent experiments. One-way ANOVA was used for statistical analysis among the different groups. Ns no significance, *p < 0.05, **p < 0.01, ***p < 0.0001, ****p < 0.0001.

further support that LRRK2 overexpression leads to the perturbation of mitochondrial homeostasis with more fragmentation where MFN2 levels are down-regulated.

It has been previously reported that MFN2 underwent degradation through ubiquitination in response to cellular stress [45]. In HK-2-*LRRK2* cells we have observed more ubiquitination of MFN2 protein (Fig. 5d). Proteasome inhibitor MG132 (Fig. 5e) treatment completely eliminated the difference in MFN2 levels. In addition, phosphorylation of $MFN2^{T111/S442}$ by PINK1 [46,47] or phosphorylation of $MFN2^{Ser27}$ by JNK [45] results in ubiquitin-mediated degradation of MFN2. We found that inhibition of PINK1 by 3-methyladenine (3-MA) could not save the loss of MFN2 in HK-2-*LRRK2* cells (Figs. S6d–e). We also did not observe the difference of mitophagy between $Lrrk2^{-/-}$ and WT mice (Figs. S6a–f), which means that the degradation of MFN2 is PINK1-PARKIN independent. When we immunoprecipitated MFN2 and immunoblotted with an antibody that recognized phosphorylated $MFN2^{Ser27}$ (S*PXR/K [(*) represents Ser phosphorylation]) [45], we observed that phosphorylation of MFN2 ^{Ser27} was apparently higher in HK-2-*LRRK2* cells and a remarkable increase further with the addition of MG132 (Fig. 5f). These results indicate that LRRK2 promotes MFN2 degradation through ubiquitination accompanied by Ser27 phosphorylation of MFN2.

LRRK2 has been reported to belong to a family member of MAPKKKs, which can phosphorylate downstream MAPK kinase (MKK) [48]. We thereafter determined whether JNK has been activated with the overexpression of LRRK2 to regulate MFN2 levels. In HK-2-*LRRK2* cells, we have observed phosphorylation of MKK4 and JNK with more extent after I/R (Fig. 5g). Moreover, treatment of a JNK inhibitor SP600125 significantly increased the protein levels of MFN2 after I/R, indicating that the degradation of MFN2 was JNK-dependent (Fig. 5h). These results demonstrated that increased MFN2 degradation in HK-2-*LRRK2* cells was MKK4/JNK dependent.

To confirm the critical roles of MFN2 in promoting LRRK2-mediating HK-2 cell impairment, HK-2 cells were co-transfected with *LRRK2* and *MFN2* and subjected to I/R. As shown in Fig. 5i, *MFN2* overexpression in HK-2-*LRRK2* cells increased cell viability to similar levels of HK-2-Vector cells after I/R. *MFN2* co-transfection suppressed the generation of mtROS upon I/R mimicry treatment (Fig. 5j) and loss of membrane potential (Fig. 5k-l). Less fragmented mitochondria were detected in HK-2-*LRRK2* cells co-transfected with *MFN2* after I/R (Fig. 5m-n). All these results indicate that LRRK2 promotes ubiquitination-mediated MFN2 degradation through phosphorylation of Ser27 in the MKK4/JNK-dependent pathway, which in turn promotes mitochondrial injury upon I/R.

2.7. LRRK2 enzymatic activity promotes the apoptosis of HK-2 cells with decreased MFN2 levels and more mitochondrial injury exposed to in vitro I/R treatment

Next, we explored whether the kinase activity of LRRK2 could influence the activation of the MKK4/JNK pathway and MFN2 degradation. Notably, LRRK2 kinase inhibitors (LRRK2-IN-1 and MLi-2) attenuated MFN2 loss after I/R (Fig. 6a) and reduced the phosphorylation of MFN2 (Fig. 6b). To further confirm the influence of LRRK2 kinase activity, we generated $LRRK2^{G2019S}$ (kinase activated) and $LRRK2^{D1994A}$ (kinase dead) mutations and transfected them into HK-2 cells. $LRRK2^{G2019S}$ further reduced cell viability while $LRRK2^{D1994A}$ alleviated the injury after I/R (Fig. 6c). Consistently, HK-2-$LRRK2^{G2019S}$ cells displayed higher mtROS levels and mitochondrial transmembrane potential loss while HK-2-$LRRK2^{D1994A}$ cells showed less severe mitochondrial injury (Fig. 6d–e). Furthermore, $LRRK2^{G2019S}$ aggravated the loss of MFN2 while $LRRK2^{D1994A}$ attenuated the loss of MFN2 (Fig. 6f) when compared to HK-2-*LRRK2* cells. $LRRK2^{G2019S}$ also led to higher phosphorylation of $MFN2^{Ser27}$ while $LRRK2^{D1994A}$ failed to increase MFN2 phosphorylation (Fig. 6g). These results indicate the critical roles of LRRK2 enzymatic activity in modulating mitochondrial dynamics through regulating MFN2 expression.

2.8. $Lrrk2^{-/-}$ mice are more resistant to fibrosis formation after acute kidney injury

Since mitochondrial dysfunction also plays a core role in dictating renal recovery and fibrosis responses following acute injury [49], we investigated whether LRRK2 also promoted AKI to CKD transition. 12 weeks after acute I/R injury, $Lrrk2^{-/-}$ mice showed less severe kidney dysfunction with lower amounts of sCr and BUN (Fig. 7a–c). Lower levels of Collagen III and α-smooth muscle actin (α-SMA) (Fig. 7d) were expressed in the kidneys from $Lrrk2^{-/-}$ mice, which were also confirmed by Masson staining and immunostaining (Fig. 7e–h).

In the cisplatin-induced AKI-CKD model (Fig. 7i), all $Lrrk2^{-/-}$ mice survived within 28 days whereas WT mice had much higher mortality (Fig. 7j). Similarly, BUN was lower in $Lrrk2^{-/-}$ mice after cisplatin injection (Fig. 7k). Urine albumin-creatinine ratio (ACR), an indicator of kidney dysfunction, was also lower in $Lrrk2^{-/-}$ mice than (Fig. 7l). There was less collagen volume fraction and α-SMA expression (Fig. 7m-p) in the kidneys from $Lrrk2^{-/-}$ mice.

We also investigated the role of *Lrrk2* in unilateral ureteral obstruction (UUO) (Fig. 7q). Similarly, we found less collagen III deposition, α-SMA expression, and less severe kidney injury in $Lrrk2^{-/-}$ mice (Fig. 7r–v). Based on staining, collagens were less deposited in the kidneys from $Lrrk2^{-/-}$ mice after UUO (Fig. 7u,7w-x), while no difference was found in α-SMA staining (Fig. 7u and y), These results indicate that deficiency in *Lrrk2* retards AKI-to-CKD transition with less fibrosis in the kidneys.

2.9. Inhibition of LRRK2 activity alleviates acute kidney injury and chronic kidney fibrosis

We next explored whether commercial LRRK2 inhibitors could be efficient in improving kidney injury. Two LRRK2 inhibitors LRRK2-IN-1

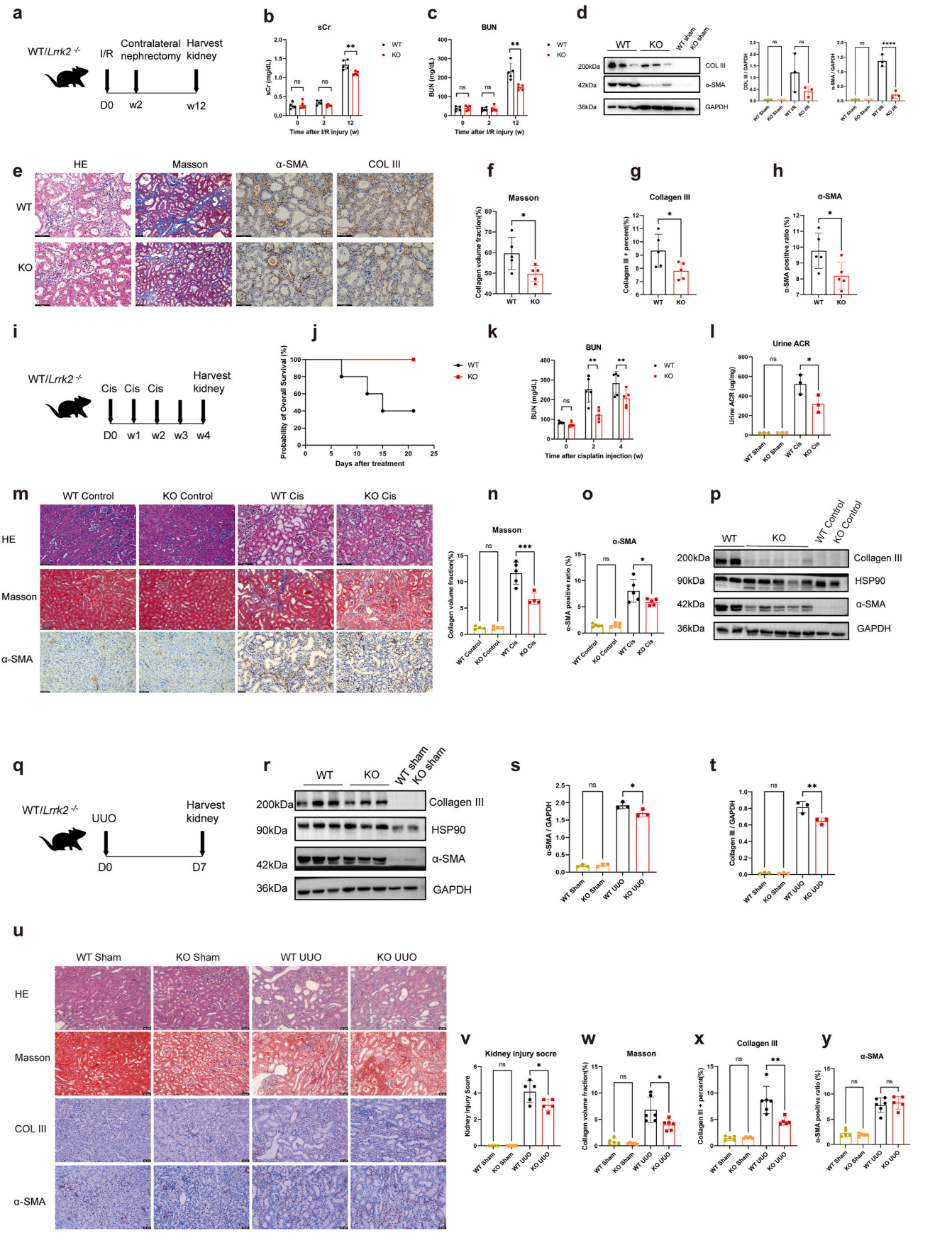

(caption on next page)

Fig. 7. *Lrrk2*$^{-/-}$ mice are more resistant to fibrosis formation after acute kidney.
(a) Experimental scheme of I/R-induced AKI-CKD model.
(**b-c**) Comparisons of sCr (a) and BUN (b) dynamics in WT and *Lrrk2*$^{-/-}$ mice after I/R injury (n = 5/group).
(**d**) Immunoblotting analysis and quantification of collagen III and α-SMA in sham and I/R kidneys from WT and *Lrrk2*$^{-/-}$ mice.
(**e-h**) Representative images of H&E staining (e) and comparisons of total collagen deposition by Masson staining (f), collagen III deposition (g), and α-SMA (h) in the kidneys from WT and *Lrrk2*$^{-/-}$ mice at 12 weeks after I/R injury (n = 5/group, n = 10 fields/section). Scale bar: 100 μm
(**i**) Experimental scheme of cisplatin-induced AKI-CKD model.
(**j**) Overall survival of WT and *Lrrk2*$^{-/-}$ mice after cisplatin injection (n = 5/group).
(**k**) sCr dynamics in WT and *Lrrk2*$^{-/-}$ mice after cisplatin injection (n = 5/group).
(**l**) Urine albumin-creatinine ratio of WT and *Lrrk2*$^{-/-}$ mice at 4 weeks after cisplatin injection (n = 5/group).
(**m-o**) Representative Masson staining and α-SMA immunostaining of the kidneys and quantification (n = 10 fields/section) 4 weeks after cisplatin injection. Scale bar: 50 μm. (**p**) Immunoblot analysis of collagen III and α-SMA in cisplatin-injured mouse kidneys from WT and *Lrrk2*$^{-/-}$ mice.
(q) Experimental scheme of UUO-induced AKI-CKD model.
(**r-t**) Immunoblot analysis and quantification of collagen III and α-SMA in UUO injured mouse kidneys from WT and *Lrrk2*$^{-/-}$ mice.
(**u-y**) Representative images of H&E staining(o) to detect kidney injury scores (p), Masson staining to detect total collagen deposition (q), collagen III immunostaining (r), and α-SMA immunostaining (s) of the kidneys from WT and *Lrrk2*$^{-/-}$ mice at 7 days after UUO injury. Quantification was performed respectively (n = 10 fields/section). Scale bar: 50 μm.
Abbreviations: sCr serum creatinine, *BUN* blood urea nitrogen, *WT* wild type, *KO Lrrk2*$^{-/-}$, *I/R* ischemia/reperfusion, *Cis* cisplatin, *COL3* collagen III, *UUO* unilateral ureteral obstruction, *α-SMA* α-smooth muscle actin
All the pooled data were presented as mean ± SD. The data were representative of two independent experiments. A *Student's t*-test was used for statistical analysis between two groups. Ns: no significance. *p < 0.05,**p < 0.01, ****p < 0.0001, ns: no significance.

and MLi-2 have been used before I/R-induced AKI and cisplatin-induced AKI-CKD (Fig. 8a). It was apparent that BUN, sCr, and serum KIM-1levels were significantly lower upon LRRK2-IN-1 and MLi-2 treatment (Fig. 8b–d) 24 h after I/R with lower kidney injury score, reduced TUNEL^{+} cells, and lower KIM-1 expression in the kidneys (Fig. 8e–h). *In vivo* treatment of LRRK2 inhibitors also reduced the loss of MFN2 with lower ROS levels and less mitochondrial fragmentation according to TEM observation (Fig. 8e and 8i-k). LRRK2-IN-1 and MLi-2 treatment also reduced kidney fibrosis 4 weeks after cisplatin treatment with lower kidney injury score, less collagen volume fractions, α-SMA expression, and collagen III deposition (Fig. 8l-p). These data further demonstrate that inhibition of LRRK2 activity before injury can alleviate acute and chronic kidney injury accompanied by ameliorating mitochondrial defects.

3. Discussion

Mitochondria have been extensively demonstrated to be involved in the pathogenesis of AKI and CKD where mitochondrial homeostasis is perturbed through multiple mechanisms [9]. In this study, we have identified LRRK2 as a novel modulator to aggravate AKI and associated fibrosis through promoting MFN2 degradation. Consequently, mitochondrial dynamics were interrupted with more fragmented mitochondria together with increased mtROS levels. Mechanically, LRRK2 activated MKK4/JNK to phosphorylate MFN2^{Ser27} for subsequent ubiquitination and degradation. Our study thus proposes LRRK2 as a novel intervention target to relieve AKI severity and retard associated profibrotic responses.

Proper mitochondrial dynamic transformation through fusion and fission is critical to maintaining mitochondrial population in a healthy status. Previous studies have reported that mitochondrial fragmentation occurred prior to tubular cell apoptosis and inhibition of fission attenuated tubular cell death and kidney injury [50]. Consistently, proximal tubule-specific deletion of *Drp1* protected the mice from severe I/R-induced AKI through reducing tubular cell death and kidney injury [51]. In this study, we have revealed an alternative mechanism of mitochondrial dynamics in AKI where mitochondria fusion was reno-protective against AKI and subsequent fibrosis. It has been well demonstrated that extra mitochondria fission could generate more mitochondria fragmentation and increased ROS, which could promote tissue damage during AKI [9]. On the contrary, mitochondria fusion is more likely to fulfill functional implementation among mitochondria networks, and sometimes reduce harmful molecules such as ROS to release organelle stress [52]. During kidney injury, the increase in fusion could meet the energetic and metabolic requirement for tissue repair to more extent.

MFN2 is reported to be involved in another mitochondrial quality control process of mitophagy by the PARKIN-PINK1 axis to remove defective mitochondria [47], which is also one of the pathogenic mechanisms of AKI [53–55]. In fetal cardiomyocytes PINK1 phosphorylates MFN2^{S442}, enabling its binding to PARKIN for the induction of mitophagy [46,47]. However, in our study, we did not observe the difference in mitophagy between *Lrrk2*$^{-/-}$ and WT mice (Figs. S7a–f). Inhibition of PARKIN did not rescue the loss of MFN2 either (Figs. S6d–e). It has been reported that loss of LRRK2 causes age-dependent alterations of the autophagic activity in *Lrrk2*$^{-/-}$ kidneys, which is unchanged at 1 month of age, enhanced at 7 months but reduced at 20 months [29]. In our study, we didn't observe differences in LC3 and p62 between WT and *Lrrk2*$^{-/-}$ kidneys, which may be because the difference is not obvious in 3-month mice.

Alternatively, we have detected the phosphorylation of MFN2 by JNK, which was activated by upstream MKK, a substrate of LRRK2 [48,56]. Although both JNK and PINK1 could phosphorylate MFN2, the serine sites of the two enzymes are not the same. While PINK1 is reported to phosphorylate MFN2^{S422} [46,47], JNK is more likely to phosphorylate MFN2^{S27} [45]. In response to cellular stress, MFN2 is phosphorylated by JNK, leading to the recruitment of another E3 ubiquitin ligase Huwe1 to MFN2 and subsequent ubiquitination and degradation [45]. This process is more likely to promote the death of PTCs. We therefore propose that during AKI, LRRK2 in renal tubular cells would facilitate to active MKK/JNK axis in the cytosol, which further phosphorylates MFN2 at Ser27 site.

LRKK2 is able to regulate macrophage function against Salmonella Typhimurium infection [57] and adaptive immunity in some autoimmune diseases [58]. Interestingly, in our study, we have excluded the engagement of immune cells in LRRK2-mediated severity of AKI. One of the possibilities is that PTCs with *Lrrk2* deficiency are more sensitive to damage stimuli and thereafter undergo cell injury at the early stage of experiment AKI whereas impaired immune responses participate in AKI in the late stage. Using conditional *Lrrk2*$^{-/-}$ mice will further clarify the roles of LRRK2 in different cell types to affect the severity of AKI and associated fibrosis.

Interestingly, we have observed the fluctuated dynamics of LRRK2 expression during experimental AKI (Fig. 1b). At the steady state, LRRK2 is highly expressed in renal tubular cells which probably restrains MFN2 protein level to maintain the homeostasis of mitochondrial network. Once undergoing I/R or other stimuli shock leading to kidney injury, LRRK2 expression is firstly down-regulated which will initiate mitochondria dynamics adaptation to stabilize MFN2 proteins for fusion processes. This process will help renal tubular cells to undergo metabolic

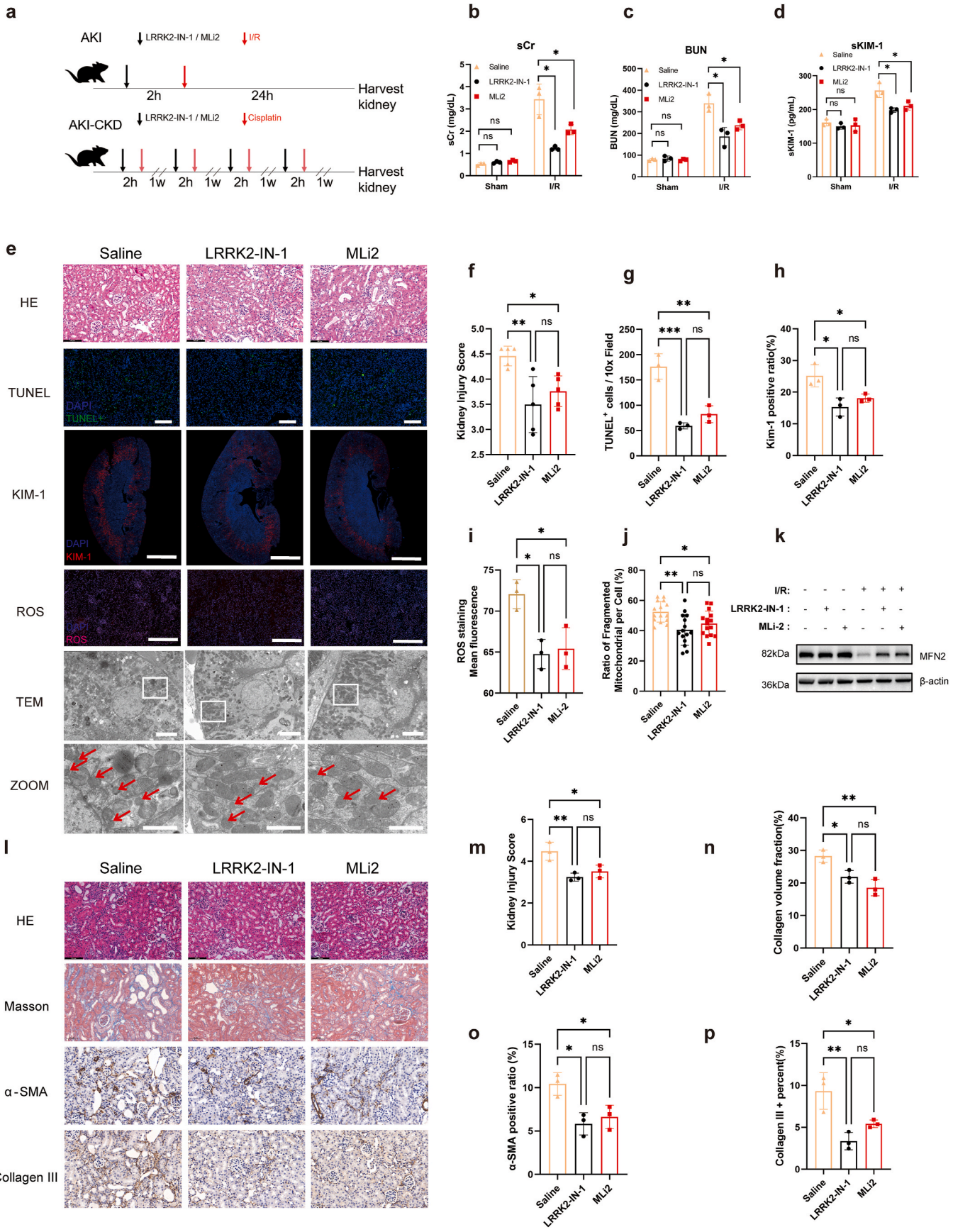

(caption on next page)

Fig. 8. LRRK2 inhibitors alleviate kidney injury in AKI *in vivo*
(a) Scheme of LRRK2 inhibitors administration and experimental design. In the AKI model, WT mice were treated with LRRK2-IN-1 (100 mg/kg, i.p) or MLi-2 (10 mg/kg, i.g) 2 h prior to I/R (n = 3/group). In the AKI-CKD model, WT mice were treated with cisplatin (10 mg/kg, i.p) weekly for consecutive 4 weeks. LRRK2-IN-1 (100 mg/kg, i.p) or MLi-2 (10 mg/kg, i.g) were administrated 2 h before every cisplatin injection.
(**b-d**) Comparisons of sCr (b), BUN (c), and serum KIM-1(d) at 24 h after I/R injury.
(**e**) Representative images of H&E staining (first lane, scale bar: 100 μm), TUNEL (second lane, scale bar: 200 μm), KIM-1 (third lane, scale bar: 50 μm), ROS (fourth lane, scale bar: 200 μm) and TEM assay (fifth lane, scale bar: 5 μm. Sixth lane, scale bar: 2 μm, red arrows showed the fragmented mitochondrial) of the kidneys at 24 h after I/R injury with or without LRRK2 inhibitor treatment.
(**f-j**) Quantification of kidney injury score (f), $TUNEL^+$ cells (g), KIM-1 positive ratio (h), ROS production (i), and the ratios of fragmented mitochondria (j) in the kidneys at 24 h after I/R injury with or without LRRK2 inhibitor treatment.
(**k**) Immunoblot analysis of MFN2 in mice kidneys treated with or without LRRK2 inhibitors.
(**l-p**) Representative images of H&E, Masson, α-SMA, and Collagen III staining of the kidneys (l) and quantification (m-p, n = 10 fields/section) at 4 weeks after cisplatin injection. Scale bar: 100 μm.
Abbreviations AKI acute kidney injury, *CKD* chronic kidney diseases, *KIM-1* kidney injury molecular 1, *ROS* reactive oxygen species, *TEM* Transmission electron microscope, *I/R* ischemia/reperfusion, *BUN* blood urea nitrogen, *sCr* serum creatinine, *WT* wild-type, *MFN2* mitofusin 2, *α-SMA* α-smooth muscle actin, *i.p* intraperitoneal injection, *i.g* intragastric administration
All the pooled data were presented as mean ± SD. The data were representative of three independent experiments. One-way ANOVA was used for statistical analysis among the different groups. *$p < 0.05$,**$p < 0.01$, ***$p < 0.001$, ns: no significance. (For interpretation of the references to colour in this figure legend, the reader is referred to the Web version of this article.)

adaption for cell proliferation and tissue repair. When AKI has been developed, LRRK2 has been observed up-regulated, which should inhibit excessive fusion and promote clearance of apoptotic PTCs [59]. Although LRRK2 is dramatically downregulated with injury, we still found LRRK2 knockout could significantly alleviate the severity of kidney injury. This may be because although the down-regulation of *Lrrk2* gene expression is quick, the degradation of LRRK2 protein is slower, which needs more than 24 h (Fig. 1c–d). LRRK2, which has not yet been reduced during the first 24 h, is sufficient to affect the prognosis of kidney damage. Therefore, pretreatment of inhibitors disturbing LRRK2 activity should be effective in alleviating the severity of AKI and associated fibrosis.

In summary, our study has revealed an alternative mitochondria-related mechanism of AKI where MFN2-mediated fusion should be reno-protective against AKI and subsequent fibrosis. LRRK2 is unfavorable to relieving the severity of kidney injury largely through promoting MFN2 degradation and impaired mitochondria fusion process. LRRK2 therefore might become a new target for preventing AKI and associated fibrosis in clinical practice.

Ethics statement

All animal experiments complied with the ARRIVE guidelines. All procedures performed in this study were in accordance with the ethical standards of the Ethics Committee of Xinhua Hospital and with the 1964 Helsinki Declaration and its later amendments or comparable ethical standards. Informed consent forms were obtained from every patient.

Funding

This work was supported by the National Natural Science Foundation of China (No. 82000638).

Authors' contributions

S Zhang: study design, perform the experiments, data analysis, manuscript writing, and editing. SB Qian: study design, supervision, providing funding, manuscript writing, and editing. HL Liu &; D Xu: study design, data analysis, manuscript writing, and editing. WM Xia and HQ Duan: help with performing the experiments, and data analysis. C Wang & SG Yu: help with data analysis. YY Chen, P Ji, and SJ Wang: giving directions and help with the experiments. XG Cui: giving directions, providing clinical specimens, and supervision. Y Wang and HB Shen: study design, data analysis, manuscript writing, editing, and supervision.

All authors have read and approved the manuscript.

Data sharing statement

Raw data from Figures were deposited on Mendeley data at https://doi.org/10.17632/s7jndhxn7k.1(https://data.mendeley.com/datasets/s7jndhxn7k/draft?a=260c1721-1028-46bb-a29e-16ff249e5401). The original western blots are given in supplemental material.

Declaration of competing interest

The authors declare that they have no conflict of interest.

Data availability

I have shared the link to my data at Date Sharing Statement in the manuscript.

Acknowledgments

We thank Department of Pathology of Xinhua Hospital for helping with histologic damage scoring, and Department of Nephrology of Xinhua Hospital for providing renal puncture samples of AKI patients. We appreciated Dr. Chuan-xin Huang from Shanghai Institute of Immunology to provide helpful comments on the manuscript, and Core Facility of Basic Medical Sciences in Shanghai Jiao Tong University College of Basic Medical Science for technical support.

Appendix A. Supplementary data

Supplementary data to this article can be found online at https://doi.org/10.1016/j.redox.2023.102860.

References

[1] A. Vijayan, Tackling AKI: prevention, timing of dialysis and follow-up, Nat. Rev. Nephrol. 17 (2) (2021) 87–88.
[2] C. Ronco, R. Bellomo, J.A. Kellum, Acute kidney injury, Lancet 394 (10212) (2019) 1949–1964.
[3] S. Kumar, Cellular and molecular pathways of renal repair after acute kidney injury, Kidney Int. 93 (1) (2018) 27–40.
[4] S.G. Coca, S. Singanamala, C.R. Parikh, Chronic kidney disease after acute kidney injury: a systematic review and meta-analysis, Kidney Int. 81 (5) (2012) 442–448.
[5] L. De Chiara, C. Conte, G. Antonelli, E. Lazzeri, Tubular cell cycle response upon AKI: revising old and new paradigms to identify novel targets for CKD prevention, Int. J. Mol. Sci. 22 (20) (2021).
[6] A.A. Sharfuddin, B.A. Molitoris, Pathophysiology of ischemic acute kidney injury, Nat. Rev. Nephrol. 7 (4) (2011) 189–200.
[7] L. Moonen, P.C. D'Haese, B.A. Vervaet, Epithelial cell cycle behaviour in the injured kidney, Int. J. Mol. Sci. 19 (7) (2018).
[8] L. Yang, T.Y. Besschetnova, C.R. Brooks, J.V. Shah, J.V. Bonventre, Epithelial cell cycle arrest in G2/M mediates kidney fibrosis after injury, Nat. Med. (N. Y., NY, U. S.) 16 (5) (2010) 535–543, 531pp. following 143.

[9] C. Tang, J. Cai, X.M. Yin, J.M. Weinberg, M.A. Venkatachalam, Z. Dong, Mitochondrial quality control in kidney injury and repair, Nat. Rev. Nephrol. 17 (5) (2021) 299–318.

[10] M. Giacomello, A. Pyakurel, C. Glytsou, L. Scorrano, The cell biology of mitochondrial membrane dynamics, Nat. Rev. Mol. Cell Biol. 21 (4) (2020) 204–224.

[11] M. Liesa, O.S. Shirihai, Mitochondrial dynamics in the regulation of nutrient utilization and energy expenditure, Cell Metabol. 17 (4) (2013) 491–506.

[12] C.A. Galloway, H. Lee, S. Nejjar, B.S. Jhun, T. Yu, W. Hsu, Y. Yoon, Transgenic control of mitochondrial fission induces mitochondrial uncoupling and relieves diabetic oxidative stress, Diabetes 61 (8) (2012) 2093–2104.

[13] S.Y. Jeong, D.W. Seol, The role of mitochondria in apoptosis, BMB Rep 41 (1) (2008) 11–22.

[14] Y. Li, H. Chen, Q. Yang, L. Wan, J. Zhao, Y. Wu, J. Wang, Y. Yang, M. Niu, H. Liu, et al., Increased Drp1 promotes autophagy and ESCC progression by mtDNA stress mediated cGAS-STING pathway, J. Exp. Clin. Cancer Res. 41 (1) (2022) 76.

[15] M. Jiang, M. Bai, J. Lei, Y. Xie, S. Xu, Z. Jia, A. Zhang, Mitochondrial dysfunction and the AKI-to-CKD transition, Am. J. Physiol. Ren. Physiol. 319 (6) (2020) F1105–f1116.

[16] Y. Sato, M. Takahashi, M. Yanagita, Pathophysiology of AKI to CKD progression, Semin. Nephrol. 40 (2) (2020) 206–215.

[17] M.R. Cookson, The role of leucine-rich repeat kinase 2 (LRRK2) in Parkinson's disease, Nat. Rev. Neurosci. 11 (12) (2010) 791–797.

[18] M. Madureira, N. Connor-Robson, R. Wade-Martins, LRRK2: autophagy and lysosomal activity, Front. Neurosci. 14 (2020) 498.

[19] E. Tolosa, M. Vila, C. Klein, O. Rascol, LRRK2 in Parkinson disease: challenges of clinical trials, Nat. Rev. Neurol. 16 (2) (2020) 97–107.

[20] J.Z. Liu, S. van Sommeren, H. Huang, S.C. Ng, R. Alberts, A. Takahashi, S. Ripke, J. C. Lee, L. Jostins, T. Shah, et al., Association analyses identify 38 susceptibility loci for inflammatory bowel disease and highlight shared genetic risk across populations, Nat. Genet. 47 (9) (2015) 979–986.

[21] C.G. Weindel, S.L. Bell, K.J. Vail, K.O. West, K.L. Patrick, R.O. Watson, LRRK2 maintains mitochondrial homeostasis and regulates innate immune responses to Mycobacterium tuberculosis, Elife 9 (2020).

[22] D. Wang, L. Xu, L. Lv, L.Y. Su, Y. Fan, D.F. Zhang, R. Bi, D. Yu, W. Zhang, X.A. Li, et al., Association of the LRRK2 genetic polymorphisms with leprosy in Han Chinese from Southwest China, Gene Immun. 16 (2) (2015) 112–119.

[23] F. Wauters, T. Cornelissen, D. Imberechts, S. Martin, B. Koentjoro, C. Sue, P. Vangheluwe, W. Vandenberghe, LRRK2 mutations impair depolarization-induced mitophagy through inhibition of mitochondrial accumulation of RAB10, Autophagy 16 (2) (2020) 203–222.

[24] H. Liu, P.W. Ho, C.T. Leung, S.Y. Pang, E.E.S. Chang, Z.Y. Choi, M.H. Kung, D. B. Ramsden, S.L. Ho, Aberrant mitochondrial morphology and function associated with impaired mitophagy and DNM1L-MAPK/ERK signaling are found in aged mutant Parkinsonian LRRK2(R1441G) mice, Autophagy 17 (10) (2021) 3196–3220.

[25] Y. Tian, J. Lv, Z. Su, T. Wu, X. Li, X. Hu, J. Zhang, L. Wu, LRRK2 plays essential roles in maintaining lung homeostasis and preventing the development of pulmonary fibrosis, Proc. Natl. Acad. Sci. U.S.A. 118 (35) (2021).

[26] M.C. Herzig, C. Kolly, E. Persohn, D. Theil, T. Schweizer, T. Hafner, C. Stemmelen, T.J. Troxler, P. Schmid, S. Danner, et al., LRRK2 protein levels are determined by kinase function and are crucial for kidney and lung homeostasis in mice, Hum. Mol. Genet. 20 (21) (2011) 4209–4223.

[27] Y. Liu, C. Hao, W. Zhang, Y. Liu, S. Guo, R. Li, M. Peng, Y. Xu, X. Pei, H. Yang, et al., Leucine-rich repeat kinase-2 deficiency protected against cardiac remodelling in mice via regulating autophagy formation and degradation, J. Adv. Res. 37 (2022) 107–117.

[28] Y. Tong, H. Yamaguchi, E. Giaime, S. Boyle, R. Kopan, R.J. Kelleher 3rd, J. Shen, Loss of leucine-rich repeat kinase 2 causes impairment of protein degradation pathways, accumulation of alpha-synuclein, and apoptotic cell death in aged mice, Proc. Natl. Acad. Sci. U.S.A. 107 (21) (2010) 9879–9884.

[29] Y. Tong, E. Giaime, H. Yamaguchi, T. Ichimura, Y. Liu, H. Si, H. Cai, J. V. Bonventre, J. Shen, Loss of leucine-rich repeat kinase 2 causes age-dependent bi-phasic alterations of the autophagy pathway, Mol. Neurodegener. 7 (2012) 2.

[30] R. Boddu, T.D. Hull, S. Bolisetty, X. Hu, M.S. Moehle, J.P. Daher, A.I. Kamal, R. Joseph, J.F. George, A. Agarwal, et al., Leucine-rich repeat kinase 2 deficiency is protective in rhabdomyolysis-induced kidney injury, Hum. Mol. Genet. 24 (14) (2015) 4078–4093.

[31] K.M. Park, J.Y. Byun, C. Kramers, J.I. Kim, P.L. Huang, J.V. Bonventre, Inducible nitric-oxide synthase is an important contributor to prolonged protective effects of ischemic preconditioning in the mouse kidney, J. Biol. Chem. 278 (29) (2003) 27256–27266.

[32] L. Yang, C.R. Brooks, S. Xiao, V. Sabbisetti, M.Y. Yeung, L.L. Hsiao, T. Ichimura, V. Kuchroo, J.V. Bonventre, KIM-1-mediated phagocytosis reduces acute injury to the kidney, J. Clin. Invest. 125 (4) (2015) 1620–1636.

[33] S. Wang, J. Fan, X. Mei, J. Luan, Y. Li, X. Zhang, W. Chen, Y. Wang, G. Meng, D. Ju, Interleukin-22 attenuated renal tubular injury in aristolochic acid nephropathy via suppressing activation of NLRP3 inflammasome, Front. Immunol. 10 (2019) 2277.

[34] M. Lech, C. Römmele, R. Gröbmayr, H. Eka Susanti, O.P. Kulkarni, S. Wang, H. J. Gröne, B. Uhl, C. Reichel, F. Krombach, et al., Endogenous and exogenous pentraxin-3 limits postischemic acute and chronic kidney injury, Kidney Int. 83 (4) (2013) 647–661.

[35] D. Katagiri, Y. Hamasaki, K. Doi, K. Negishi, T. Sugaya, M. Nangaku, E. Noiri, Interstitial renal fibrosis due to multiple cisplatin treatments is ameliorated by semicarbazide-sensitive amine oxidase inhibition, Kidney Int. 89 (2) (2016) 374–385.

[36] R.L. Chevalier, M.S. Forbes, B.A. Thornhill, Ureteral obstruction as a model of renal interstitial fibrosis and obstructive nephropathy, Kidney Int. 75 (11) (2009) 1145–1152.

[37] Y. Kirita, H. Wu, K. Uchimura, P.C. Wilson, B.D. Humphreys, Cell profiling of mouse acute kidney injury reveals conserved cellular responses to injury, Proc. Natl. Acad. Sci. U.S.A. 117 (27) (2020) 15874–15883.

[38] S. Qian, W. Xia, Y. Wu, Q. Cao, Y. Ding, Y. Huang, H. Shen, Urinary kidney injury molecule-1: a novel biomarker to monitor renal function in patients with unilateral ureteral obstruction, Int. Urol. Nephrol. 52 (11) (2020) 2065–2072.

[39] H.K. Eltzschig, T. Eckle, Ischemia and reperfusion–from mechanism to translation, Nat. Med. (N. Y., NY, U. S.) 17 (11) (2011) 1391–1401.

[40] S.C. Huen, L.G. Cantley, Macrophages in renal injury and repair, Annu. Rev. Physiol. 79 (2017) 449–469.

[41] E. Xu, R. Boddu, H.A. Abdelmotilib, A. Sokratian, K. Kelly, Z. Liu, N. Bryant, S. Chandra, S.M. Carlisle, E.J. Lefkowitz, et al., Pathological α-synuclein recruits LRRK2 expressing pro-inflammatory monocytes to the brain, Mol. Neurodegener. 17 (1) (2022) 7.

[42] C.G. Weindel, E.L. Martinez, X. Zhao, C.J. Mabry, S.L. Bell, K.J. Vail, A.K. Coleman, J.J. VanPortfliet, B. Zhao, A.R. Wagner, et al., Mitochondrial ROS promotes susceptibility to infection via gasdermin D-mediated necroptosis, Cell 185 (17) (2022) 3214–3231, e3223.

[43] D.C. Chan, Mitochondrial dynamics and its involvement in disease, Annu. Rev. Pathol. 15 (2020) 235–259.

[44] M.J. Livingston, J. Wang, J. Zhou, G. Wu, I.G. Ganley, J.A. Hill, X.M. Yin, Z. Dong, Clearance of damaged mitochondria via mitophagy is important to the protective effect of ischemic preconditioning in kidneys, Autophagy 15 (12) (2019) 2142–2162.

[45] G.P. Leboucher, Y.C. Tsai, M. Yang, K.C. Shaw, M. Zhou, T.D. Veenstra, M. H. Glickman, A.M. Weissman, Stress-induced phosphorylation and proteasomal degradation of mitofusin 2 facilitates mitochondrial fragmentation and apoptosis, Mol. Cell 47 (4) (2012) 547–557.

[46] Y. Chen, G.W. Dorn 2nd, PINK1-phosphorylated mitofusin 2 is a Parkin receptor for culling damaged mitochondria, Science 340 (6131) (2013) 471–475.

[47] G. Gong, M. Song, G. Csordas, D.P. Kelly, S.J. Matkovich, G.W. Dorn 2nd, Parkin-mediated mitophagy directs perinatal cardiac metabolic maturation in mice, Science 350 (6265) (2015) aad2459.

[48] C.Y. Chen, Y.H. Weng, K.Y. Chien, K.J. Lin, T.H. Yeh, Y.P. Cheng, C.S. Lu, H. L. Wang, (G2019S) LRRK2 activates MKK4-JNK pathway and causes degeneration of SN dopaminergic neurons in a transgenic mouse model of PD, Cell Death Differ. 19 (10) (2012) 1623–1633.

[49] X. Zhang, E. Agborbesong, X. Li, The role of mitochondria in acute kidney injury and chronic kidney disease and its therapeutic potential, Int. J. Mol. Sci. (20) (2021) 22.

[50] C. Brooks, Q. Wei, S.G. Cho, Z. Dong, Regulation of mitochondrial dynamics in acute kidney injury in cell culture and rodent models, J. Clin. Invest. 119 (5) (2009) 1275–1285.

[51] H.M. Perry, L. Huang, R.J. Wilson, A. Bajwa, H. Sesaki, Z. Yan, D.L. Rosin, D. F. Kashatus, M.D. Okusa, Dynamin-related protein 1 deficiency promotes recovery from AKI, J. Am. Soc. Nephrol. 29 (1) (2018) 194–206.

[52] Y. Zhang, Y. Wang, J. Xu, F. Tian, S. Hu, Y. Chen, Z. Fu, Melatonin attenuates myocardial ischemia-reperfusion injury via improving mitochondrial fusion/mitophagy and activating the AMPK-OPA1 signaling pathways, J. Pineal Res. 66 (2) (2019), e12542.

[53] Q. Lin, S. Li, N. Jiang, X. Shao, M. Zhang, H. Jin, Z. Zhang, J. Shen, Y. Zhou, W. Zhou, et al., PINK1-parkin pathway of mitophagy protects against contrast-induced acute kidney injury via decreasing mitochondrial ROS and NLRP3 inflammasome activation, Redox Biol. 26 (2019), 101254.

[54] Y. Wang, J. Zhu, Z. Liu, S. Shu, Y. Fu, Y. Liu, J. Cai, C. Tang, Y. Liu, X. Yin, et al., The PINK1/PARK2/optineurin pathway of mitophagy is activated for protection in septic acute kidney injury, Redox Biol. 38 (2021), 101767.

[55] Z.J. Fu, Z.Y. Wang, L. Xu, X.H. Chen, X.X. Li, W.T. Liao, H.K. Ma, M.D. Jiang, T. T. Xu, J. Xu, et al., HIF-1α-BNIP3-mediated mitophagy in tubular cells protects against renal ischemia/reperfusion injury, Redox Biol. 36 (2020), 101671.

[56] Y. Zhu, C. Wang, M. Yu, J. Cui, L. Liu, Z. Xu, ULK1 and JNK are involved in mitophagy incurred by LRRK2 G2019S expression, Protein Cell 4 (9) (2013) 711–721.

[57] E. Kozina, S. Sadasivan, Y. Jiao, Y. Dou, Z. Ma, H. Tan, K. Kodali, T. Shaw, J. Peng, R.J. Smeyne, Mutant LRRK2 mediates peripheral and central immune responses leading to neurodegeneration in vivo, Brain 141 (6) (2018) 1753–1769.

[58] M. Zhang, C. Yao, J. Cai, S. Liu, X.N. Liu, Y. Chen, S. Wang, P. Ji, M. Pan, Z. Kang, et al., LRRK2 is involved in the pathogenesis of system lupus erythematosus through promoting pathogenic antibody production, J. Transl. Med. 17 (1) (2019) 37.

[59] Y. Wang, M. Subramanian, A. Yurdagul Jr., V.C. Barbosa-Lorenzi, B. Cai, J. de Juan-Sanz, T.A. Ryan, M. Nomura, F.R. Maxfield, I. Tabas, Mitochondrial fission promotes the continued clearance of apoptotic cells by macrophages, Cell 171 (2) (2017) 331–345, e322.